Microelectronics Reliability 49 (2009) 1529–1536

Contents lists available at ScienceDirect

Microelectronics Reliability

journal homepage: www.elsevier.com/locate/microrel

Fast and stable computation of optical propagation in micro-waveguides with loss

Jianxin Zhu *, Rencheng Song

Department of Mathematics, Zhejiang University, Hangzhou 310027, Zhejiang Province, China

ARTICLE INFO

Article history:
Received 11 February 2009
Received in revised form 13 June 2009
Available online 19 July 2009

ABSTRACT

The optical propagation in micro-waveguides with loss is described by Helmholtz equation with complex refractive index or wavenumber. In this paper, an improved operator marching method is developed to solve the equation efficiently. This technique can be widely used for microelectronic on-chip interconnect applications.

© 2009 Elsevier Ltd. All rights reserved.

1. Introduction

Recently, one of the major concerns for future gigascale integrated circuit technology is the interconnect issue [1–3]. Silicon oxynitride has been considered as the most promising material for this application [4] because of its tunable optical properties such as refractive index. However, high optical loss and large fluctuation of refractive index were found in the material. Numerical simulation is helpful for the modeling and design of micro-waveguides in such lossy media, where the optical propagation is controlled by the well known Helmholtz equation with complex refractive index or wavenumber.

For lossless waveguides, that is, the Helmholtz equation with real wavenumber, there is an operator marching method (OMM) [5] to compute the optical propagation efficiently. However, for the lossy waveguides, since the transverse operator of the complex Helmholtz equation is usually non-self-adjoint [6,7], its eigenfunctions are no longer orthogonal as in the lossless media. It leads to the difficulty of local base transform in OMM because of the instability in numerical implementation. Thus, the OMM algorithm [5] fails in the lossy waveguides.

In this study, the above difficulty is overcome in the improved OMM. First, two fast treatments are given to do the local base transform for lossy waveguides. Then the propagation loss is properly introduced into OMM by selecting the branch cut for the complex propagation constants. The real parts determine the change of phase velocity, and the imaginary parts control the decay of amplitude. Details will be shown in next sections.

2. Background

In this section, we first present the mathematical formulation of a lossy waveguide. Then the transverse operator of the Helmholtz equation and its characteristic problem are introduced.

2.1. The formulation of a long-distance lossy waveguide

Consider a two-dimensional homogeneous complex Helmholtz equation

$$u_{zz} + u_{xx} + \kappa^2(x,z)u = 0 \quad (1)$$

in the strip $0 < z < 1$, where x is the range direction, z is the transverse direction, and κ is the complex wavenumber which is x-invariant for $x < 0$ $(\kappa(x,z) = \kappa_0(z))$ and $x > L$ $(\kappa(x,z) = \kappa_\infty(z))$. Suppose $\mathrm{Re}(\kappa) > 0, \mathrm{Im}(\kappa) > 0, \mathrm{Im}(\kappa) \ll \mathrm{Re}(\kappa)$, and $\frac{1}{\mathrm{Re}(\kappa)} \ll 1 \ll L$. The restrictions on $\kappa(x,z)$ show that the wave propagates in the weakly lossy medium over a long distance.

The boundary condition (BC) on x-direction is

$$u(0,z) = f(z), \quad u_x(L,z) = \mathbf{i}\sqrt{\partial_z^2 + \kappa^2(L,z)}\,u(L,z), \quad (2)$$

where $f(z)$ is a given incident wave and $\mathbf{i} = \sqrt{-1}$. The square root operator of $\sqrt{\partial_z^2 + \kappa^2(L,z)}$ will be defined in Section 2.2. The BC at $x = L$ is a radiation condition. It indicates the waves propagate towards ∞ for $x > L$.

Two types of BCs on z-direction are studied. One is

$$u(x,0) = 0, \; u(x,1) = 0. \quad (3)$$

The other is

$$u(x,0) = 0, \; u_z(x,1) = 0. \quad (4)$$

The problem sketch is shown in Fig. 1.

2.2. The transverse operator of Helmholtz equation and its characteristic problem

The transverse operator of Helmholtz equation is

$$D(x) = \partial_z^2 + \kappa^2(x,z),$$

where x is fixed.

* Corresponding author.
E-mail address: zjx@zju.edu.cn (J. Zhu).

0026-2714/$ - see front matter © 2009 Elsevier Ltd. All rights reserved.
doi:10.1016/j.microrel.2009.06.004

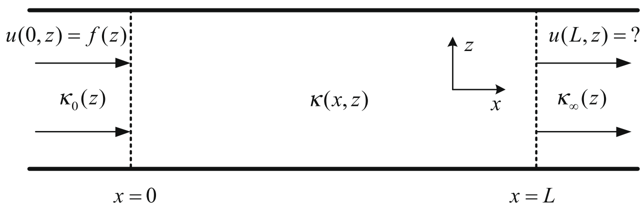

Fig. 1. The problem sketch.

The characteristic problem of $D(x)$ is important. It is defined as

$$D(x)\phi(z) = \lambda\phi(z), \quad 0 < z < 1. \tag{5}$$

Correspondingly,

$$\phi(0) = 0, \ \phi(1) = 0, \tag{6}$$

for BC (3), or

$$\phi(0) = 0, \ \frac{d\phi}{dz}(1) = 0, \tag{7}$$

for BC (4).

By multiplying Eq. (5) with ϕ^* (the complex conjugation of ϕ) and integrating it over (0,1), we have

$$\int_0^1 \kappa^2(x,z)|\phi(z)|^2 dz - \int_0^1 \left|\frac{d\phi(z)}{dz}\right|^2 dz = \lambda \int_0^1 |\phi(z)|^2 dz. \tag{8}$$

From Eq. (8), we get

$$\mathrm{Re}(\lambda) = \left(\int_0^1 \mathrm{Re}(\kappa^2(x,z))|\phi(z)|^2 dz - \int_0^1 \left|\frac{d\phi(z)}{dz}\right|^2 dz\right) \bigg/ \int_0^1 |\phi(z)|^2 dz, \tag{9}$$

$$\mathrm{Im}(\lambda) = \int_0^1 \mathrm{Im}(\kappa^2(x,z))|\phi(z)|^2 dz \bigg/ \int_0^1 |\phi(z)|^2 dz. \tag{10}$$

Thus, $\mathrm{Im}(\lambda) > 0$. Particularly, $\mathrm{Im}(\lambda) = \mathrm{Im}(\kappa^2)$ if κ^2 is z-invariant.

The square root operator $D^{\frac{1}{2}}(x) = \sqrt{\partial_z^2 + \kappa^2(x,z)}$ is defined to satisfy

$$D^{\frac{1}{2}}(x)\phi(z) = \sqrt{\lambda}\phi(z), \quad 0 < z < 1, \tag{11}$$

where $\phi(z)$ and λ are same as Eq. (5). The branch of $\sqrt{\lambda}$ is chosen as $(-\pi, \pi]$. Thus $\mathrm{Im}(\sqrt{\lambda}) > 0$ when λ is complex. The square root operator in Eq. (2) is simply $D^{\frac{1}{2}}(L)$.

Let $\{\phi_j(z)\}_{j=1}^\infty$ be a system of eigenfunctions of $D(x)$. The eigenfunction space is $L^2(0,1)$, i.e.,

$$\int_0^1 |\phi_j(z)|^2 dz < \infty, \quad j = 1, 2, \ldots, \infty.$$

The completeness and the orthogonality of $\{\phi_j(z)\}_{j=1}^\infty$ are complicated because $D(x)$ is non-self-adjoint in this study.

First, the completeness properties of $D(x)$ are listed as follows.

1. $D(x)$ for BC (6):
   (a) If the medium is lossy and homogeneous, i.e., κ is a complex constant, then $\{\phi_j(z)\}_{j=1}^\infty$ form a basis for $L^2(0,1)$ [6].
   (b) If the medium is lossy and inhomogeneous, i.e., $\kappa(x,z)$ is a complex and bounded function on (0, 1) with fixed x, then $\{\phi_j(z)\}_{j=1}^\infty$ form a basis for $L^2(0,1)$ [6,12].
2. $D(x)$ for BC (7):
   If $\mathrm{Im}(\kappa) \ll \mathrm{Re}(\kappa), D(x)$ can be treated as a perturbation of the self-adjoint operator $\widehat{D}(x) = \partial_z^2 + \mathrm{Re}(\kappa^2(x,z))$. Namely, if $\mathrm{Im}(\kappa(x,z))$ is small enough, then $\{\phi_j(z)\}_{j=1}^\infty$ form a basis for $L^2(0,1)$.

Although the property 2 of $D(x)$ for BC (7) is not rigorous, it is usually true for practical weakly lossy waveguides. Therefore, we assume $\{\phi_j(z)\}_{j=1}^\infty$ form a complete basis for $L^2(0,1)$. Namely, they are linearly independent.

Second, we study the orthogonality of $\{\phi_j(z)\}_{j=1}^\infty$. Two functions $p(z)$ and $q(z)$ are orthogonal in $L^2(0,1)$ if

$$\langle p, q\rangle = \int_0^1 p^* q dz = 0. \tag{12}$$

Though ϕ_i and ϕ_j are not orthogonal in $L^2(0,1)$, it is pointed out in [7] that

$$(\phi_i, \phi_j) = \int_0^1 \phi_i \phi_j dz = 0, \quad i \neq j, \tag{13}$$

when $D(x)$ is symmetric.

In discrete form, Eq. (13) changes to

$$(X, Y) = X^T Y = 0, \tag{14}$$

where X and Y are two different eigenvectors of the complex symmetric matrix of $D(x)$. The notation X^T denotes the transpose of X, and its conjugate transpose is denoted as X^H hereafter. Eq. (14) is an intrinsic property called complex orthogonal [8] of some complex symmetric matrices.

Obviously, the operator $D(x)$ defined in Eqs. (5) and (6) (or (5) and (7)) is symmetric. However, $D(x)$ can be asymmetric in some complicated waveguides. For example, it is not symmetric in the multi-layer planar waveguide, curved waveguide, or the waveguide with improper BC. The $\{\phi_j(z)\}_{j=1}^\infty$ are not orthogonal for asymmetric $D(x)$.

Corresponding to either symmetric or asymmetric $D(x)$, two kinds of techniques are proposed to do the local base transform quickly. The details are shown in Section 3.

3. Two fast techniques for the local base transform

The local base transform in OMM needs to be done in each marching step by searching a coordinate matrix N satisfying $V_1 = V_0 N$, where V_0 and V_1 are known eigenvector matrices of $D(x)$ at different locations. When $D(x)$ is Hermitian, N can be easily obtained by $N = V_0^H V_1$. Hence, the local base transform is easily done in lossless waveguide (κ is real), where $D(x)$ is self-adjoint.

In lossy waveguides with complex $\kappa, D(x)$ is non-self-adjoint and the eigenfunctions of $D(x)$ are not orthogonal. It makes the local base transform in OMM fail. One remedial treatment is to find the inverse matrix of V_0, i.e., $N = V_0^{-1} V_1$. It is time-consuming and unstable. However, with this connection, two techniques, namely, the complex symmetric matrix method and the adjoint operator method are described in this section.

3.1. The complex symmetric matrix method

The technique of local base transform for symmetric $D(x)$, called the complex symmetric matrix method, is introduced in this section. Denote the discretization matrix of D as M. Then M is symmetric, i.e., $M^T = M$. As $\{\phi_j(z)\}_{j=1}^\infty$ are linearly independent, M is also invertible. Hence M is a complex, symmetric, and invertible matrix.

There is an important property for this kind of matrices, see Ref. [8]. We restate it below.

Theorem 1. *An $n \times n$ complex symmetric matrix Z is diagonalizable if and only if there is an eigenvector matrix V such that*

$$V^T Z V = \Lambda = diag(\lambda_1, \lambda_2, \ldots, \lambda_n)$$

and $V^T V = I$, where I is the $n \times n$ identity matrix.

By Theorem 1, we get

$$V_0^{\mathrm{T}} M V_0 = \Lambda_0, \quad V_0^{\mathrm{T}} V_0 = I,$$

where Λ_0 is the diagonal eigenvalue matrix of M, and V_0 is its eigenvector matrix. Then $N = V_0^{\mathrm{T}} V_1$ if $V_1 = V_0 N$.

3.2. The adjoint operator method

The technique of local base transform for asymmetric $D(x)$ is introduced in this section, which is called the adjoint operator method. A bi-orthogonal set $\{\varphi_j\}_{j=1}^{\infty}$ for eigenfunctions $\{\phi_j\}_{j=1}^{\infty}$ is formed in this method. As known, $\{\varphi_j\}_{j=1}^{\infty}$ are the eigenfunctions of the adjoint operator of D.

Definition 1. The operator G is called the adjoint operator of D in $L^2(0,1)$, if

$$\langle \varphi, D\phi \rangle = \langle G\varphi, \phi \rangle, \ \text{i.e.}, \quad \int_0^1 \varphi^* D\phi \mathrm{d}z = \int_0^1 (G\varphi)^* \phi \mathrm{d}z,$$

for any φ and ϕ in $L^2(0,1)$.

This definition can be found in many textbooks of partial differential equations. The relation between D and G is reciprocal.

Taking Eqs. (5) and (7) for example, we derive the adjoint operator G for D. By Definition 1 and the integration by parts, there is

$$\int_0^1 \varphi^* D\phi \mathrm{d}z = \int_0^1 \left(\frac{\partial^2 \varphi^*}{\partial z^2} + \kappa^2 \varphi^* \right) \phi \mathrm{d}z + \varphi^* \frac{\mathrm{d}\phi}{\mathrm{d}z}\bigg|_0^1 - \frac{d\varphi^*}{\mathrm{d}z} \phi \bigg|_0^1. \tag{15}$$

Substitute Eq. (7) into Eq. (15) and let $\varphi^*(0) = 0$, $\frac{d\varphi^*}{\mathrm{d}z}(1) = 0$. We get $G = \frac{\mathrm{d}^2}{\mathrm{d}z^2} + (\kappa^2)^*$ from Definition 1. Namely,

$$\frac{d^2 \varphi}{\mathrm{d}z^2} + (\kappa^2)^* \varphi = \lambda^* \varphi, \tag{16}$$

$$\varphi(0) = 0, \tag{17}$$

$$\frac{d\varphi}{\mathrm{d}z}(1) = 0. \tag{18}$$

Similarly, the adjoint operator G of D in Eqs. (5) and (6) satisfies

$$\frac{d^2 \varphi}{\mathrm{d}z^2} + (\kappa^2)^* \varphi = \lambda^* \varphi,$$

$$\varphi(0) = 0,$$

$$\varphi(1) = 0.$$

In the following, we verify the bi-orthogonal property of $\{\varphi_j\}_{j=1}^{\infty}$ and $\{\phi_j\}_{j=1}^{\infty}$. In fact, let λ_j and λ_i be two different eigenvalues of D. Suppose

$$D\phi_i = \lambda_i \phi_i, \quad G\varphi_j = \lambda_j^* \varphi_j.$$

From Definition 1, we have

$$(\lambda_j - \lambda_i) \int_0^1 \varphi_j^* \phi_i \mathrm{d}z = 0.$$

Since $\lambda_i \neq \lambda_j$, then $\int_0^1 \varphi_j^* \phi_i \mathrm{d}z = 0$, i.e., $\langle \varphi_j, \phi_i \rangle = 0, \ i \neq j$.

In practical calculation, D and G are discretized as two matrices M and W, respectively. The eigenvector decomposition for M is first calculated

$$MV_0 = V_0 \Lambda_0.$$

Denote the eigenvector decomposition of W as

$$W\widehat{V}_0 = \widehat{V}_0 \Lambda_0^{\mathrm{H}}.$$

Then $\widehat{V}_0$ is the bi-orthogonal set of V_0, i.e.,

$$\widehat{V}_0^{\mathrm{H}} V_0 = I.$$

The unknown eigenvector matrix $\widehat{V}_0$ can be calculated by the inverse iteration method [9]. It converges quickly. Only a small additional effort is needed to solve $\widehat{V}_0$ from V_0 and Λ_0. Then $N = \widehat{V}_0^{\mathrm{H}} V_1$ if $V_1 = V_0 N$.

Obviously, the adjoint operator method can also be used for symmetric $D(x)$. However, the complex symmetric matrix method is simpler and more efficient in that case.

4. The propagation loss and improved OMM formulas

The propagation loss is introduced into OMM for lossy waveguides in Section 4.1. It can be easily understood by the relation of OMM and the coupled mode method [10]. The relation is also indicated in [11] to study a fourth order method for lossless waveguides. The improved marching formulas are given in Section 4.2.

4.1. The propagation loss

The range is divided into uniform piece-wise x-independent segments. Let the discrete points $\{x_j\}$ satisfy

$$-\infty < 0 = x_0 < x_1 < \cdots < x_N = L < +\infty.$$

Each interval (x_i, x_{i+1}) corresponds to a range-independent segment. The approximated Helmholtz equation on (x_i, x_{i+1}) is

$$u_{xx} + u_{zz} + \kappa^2(x_{i+1/2}, z) u = 0. \tag{19}$$

We take $i = 0$ for example to describe the loss of wave propagation from x_0 to x_1.

The wave field is decomposed as right- and left-going waves

$$u = u^{(+)} + u^{(-)}, \tag{20}$$

where $u^{(+)}$ and $u^{(-)}$ satisfy

$$u_x^{(+)}(x,z) = \mathbf{i} D^{\frac{1}{2}}\left(x_{\frac{1}{2}}\right) u^{(+)}(x,z), \quad u_x^{(-)}(x,z) = -\mathbf{i} D^{\frac{1}{2}}\left(x_{\frac{1}{2}}\right) u^{(-)}(x,z), \tag{21}$$

respectively, see [5]. Then

$$\int_{x_0}^{x} \frac{du^{(+)}}{u^{(+)}} = \int_{x_0}^{x} \mathbf{i} D^{\frac{1}{2}}\left(x_{\frac{1}{2}}\right) \mathrm{d}x, \quad \int_{x_1}^{x} \frac{du^{(-)}}{u^{(-)}} = \int_{x_1}^{x} -\mathbf{i} D^{\frac{1}{2}}\left(x_{\frac{1}{2}}\right) \mathrm{d}x. \tag{22}$$

We get

$$u^{(+)}(x,z) = e^{\mathbf{i} D^{\frac{1}{2}}\left(x_{\frac{1}{2}}\right)(x - x_0)} u^{(+)}(x_0, z),$$

$$u^{(-)}(x,z) = e^{-\mathbf{i} D^{\frac{1}{2}}\left(x_{\frac{1}{2}}\right)(x - x_1)} u^{(-)}(x_1, z). \tag{23}$$

Let $\{\phi_j(z)\}$ be the eigenfunctions of $D\left(x_{\frac{1}{2}}\right)$. Then

$$D\left(x_{\frac{1}{2}}\right) \phi_j(z) = \lambda_j \phi_j(z), \quad j = 1, 2 \ldots, n,$$

and

$$D^{\frac{1}{2}}\left(x_{\frac{1}{2}}\right) \phi_j(z) = \sqrt{\lambda_j} \phi_j(z), \quad j = 1, 2 \ldots, n.$$

Suppose

$$u^{(+)}(x_0, z) = \sum_{j=1}^{\infty} \alpha_j \phi_j(z), \tag{24}$$

$$u^{(-)}(x_1, z) = \sum_{j=1}^{\infty} \beta_j \phi_j(z), \tag{25}$$

where $\{\alpha_j\}$ and $\{\beta_j\}$ are the strength coefficients of right- and left-going waves, respectively. They can be determined in the coupled mode method by the interface conditions.

Substituting Eqs. (24) and (25) into Eq. (23), yields

$$u^{(+)}(x,z) = e^{\mathbf{i}D^{\frac{1}{2}}(x_{1/2})(x-x_0)}\sum_{j=1}^{\infty}\alpha_j\phi_j(z) = \sum_{j=1}^{\infty}\alpha_j e^{\mathbf{i}D^{\frac{1}{2}}(x_{1/2})(x-x_0)}\phi_j(z)$$
$$= \sum_{j=1}^{\infty}\alpha_j e^{\mathbf{i}\sqrt{\lambda_j}(x-x_0)}\phi_j(z), \qquad (26)$$

$$u^{(-)}(x,z) = e^{-\mathbf{i}D^{\frac{1}{2}}(x_{1/2})(x-x_1)}\sum_{j=1}^{\infty}\beta_j\phi_j(z)$$
$$= \sum_{j=1}^{\infty}\beta_j e^{-\mathbf{i}D^{\frac{1}{2}}(x_{1/2})(x-x_1)}\phi_j(z) = \sum_{j=1}^{\infty}\beta_j e^{-\mathbf{i}\sqrt{\lambda_j}(x-x_1)}\phi_j(z), \qquad (27)$$

where

$$e^{\mathbf{i}D^{\frac{1}{2}}(x_{1/2})(x-x_0)}\phi_j(z) = e^{\mathbf{i}\sqrt{\lambda_j}(x-x_0)}\phi_j(z),$$
$$e^{-\mathbf{i}D^{\frac{1}{2}}(x_{1/2})(x-x_1)}\phi_j(z) = e^{-\mathbf{i}\sqrt{\lambda_j}(x-x_1)}\phi_j(z).$$

From Eq. (20), we get

$$u(x,z) = \sum_{j=1}^{\infty}\left(\alpha_j e^{\mathbf{i}\sqrt{\lambda_j}(x-x_0)} + \beta_j e^{-\mathbf{i}\sqrt{\lambda_j}(x-x_1)}\right)\phi_j(z), \qquad (28)$$

which indicates that the OMM is closely related to the coupled mode method.

From the above analysis, the loss definition can be introduced into the modified OMM formulas easily. Since $\sqrt{\lambda_j} = a_j + b_j\mathbf{i}$ where $b_j > 0$, it can be seen from Eq. (28) that the wave attenuates in the lossy medium. For a given mode ϕ_j propagating from x_0 to x_1, its amplitude loss constant is $e^{-b_j(x_1-x_0)}$, while its phase factor is $e^{\mathbf{i}a_j(x_1-x_0)}$.

4.2. The formulas of the improved operator marching method

By the forward preparations, the new formulas can be obtained by a small modification of OMM in [5]. We also take the segment (x_0, x_1) for example. The marching formulas indicate the relation of operators from x_1 to x_0.

For Eqs. (5) and (6), the z axis is discretized by

$$z_j = j\delta, \qquad \delta = 1/n, \quad j = 1,2,\ldots,n.$$

The second order approximation to ∂_z^2 is

$$A = \frac{1}{\delta^2}\begin{bmatrix} -2 & 1 & & \\ 1 & \ddots & \ddots & \\ & \ddots & -2 & 1 \\ & & 1 & -2 \end{bmatrix}. \qquad (29)$$

For Eqs. (5) and (7), the z axis is discretized by

$$z_j = j\delta, \quad \delta = 1/(n+1/2), \quad j = 1,2,\ldots,n.$$

The second order approximation to ∂_z^2 are [5]

$$A = \frac{1}{\delta^2}\begin{bmatrix} -2 & 1 & & \\ 1 & \ddots & \ddots & \\ & \ddots & -2 & 1 \\ & & 1 & -1 \end{bmatrix}. \qquad (30)$$

Then the matrix approximating $D(x_{1/2}) = \partial_z^2 + \kappa^2(x_{1/2}, z)$ is

$$M = A + \begin{bmatrix} \kappa_1^2 & & & \\ & \kappa_2^2 & & \\ & & \ddots & \\ & & & \kappa_n^2 \end{bmatrix}, \qquad (31)$$

where A is the $n \times n$ matrix in Eq. (29) (or (30)) and $\kappa_j = \kappa(x_{1/2}, z_j)$. It can be seen M is complex and symmetric.

Just as that done in [5], the truncated local eigenfunction expansion is used in the improved OMM to raise the computing efficiency. In the discrete form, only the first m eigenvectors with the largest real parts (including all propagation modes and few evanescent modes) are computed. It is called the truncated local eigenvector decomposition, which can be calculated quickly by ARPACK or Matlab. Of course, other techniques [13–15] can also be used to solve these eigenvalues and eigenfunctions. However, we use the truncated local eigenvector decomposition for simplicity.

Denote the discrete matrices of $D\left(x_{\frac{1}{2}}\right)$ and $D\left(x_{\frac{3}{2}}\right)$ as M_0 and M_1, respectively. Their truncated local eigenvector decompositions are

$$M_0V_{0,m} = V_{0,m}\Lambda_{0,m}, \quad M_1V_{1,m} = V_{1,m}\Lambda_{1,m},$$

where $V_{i,m}$ $(i = 0,1)$ are the $n \times m$ eigenvector matrices and $\Lambda_{i,m}$ $(i = 0,1)$ are the $m \times m$ diagonal eigenvalue matrices.

By Theorem 1, there is

$$V_{i,m}^{\mathrm{T}}V_{i,m} = I, \quad i = 0,1.$$

The local base transform can be done by the complex symmetric matrix method as

$$N = V_{0,m}^{\mathrm{T}}V_{1,m}. \qquad (32)$$

Alternatively, the local base transform can also be done by the adjoint operator method. Denote W_0 as the discrete matrix of the adjoint operator $G\left(x_{\frac{1}{2}}\right)$. There is

$$W_0\widehat{V}_{0,m} = \widehat{V}_{0,m}\Lambda_{0,m}^{\mathrm{H}}.$$

Then

$$N = \widehat{V}_{0,m}^{H}V_{1,m}. \qquad (33)$$

This method is used when $D(x)$ is asymmetric.

Then the marching formulas from x_1 to x_0 in matrix form for lossy waveguides are

$$S = NS_1N^{-1}, \qquad (34)$$
$$P_1 = \left(\mathbf{i}\sqrt{\Lambda_{0,m}} + S\right)^{-1}\left(\mathbf{i}\sqrt{\Lambda_{0,m}} - S\right), \qquad (35)$$
$$P_0 = e^{\mathbf{i}h\sqrt{\Lambda_{0,m}}}P_1e^{\mathbf{i}h\sqrt{\Lambda_{0,m}}}, \qquad (36)$$
$$U = (I - P_0)(I + P_0)^{-1}, \qquad (37)$$
$$S_0 = \mathbf{i}\sqrt{\Lambda_{0,m}}U, \qquad (38)$$
$$Z_0 = NZ_1N^{-1}(I + P_1)e^{\mathbf{i}h\sqrt{\Lambda_{0,m}}}(I + P_0)^{-1}, \qquad (39)$$

where S_1 and Z_1 are known at x_1 and $h = x_1 - x_0$. By the marching formulas, S_0 and Z_0 at x_0 are obtained. The detailed derivation is similar as that in [5] and is omitted here. The propagating loss is introduced in the formulas by the definition of square root of $\sqrt{\Lambda_{0,m}}$. Namely,

$$\sqrt{\Lambda_{0,m}} = \begin{bmatrix} \sqrt{\lambda_1} & & & \\ & \sqrt{\lambda_2} & & \\ & & \ddots & \\ & & & \sqrt{\lambda_m} \end{bmatrix}, \qquad (40)$$

where $\mathrm{Im}\left(\sqrt{\lambda_j}\right) > 0, \ j = 1,2,\ldots,m.$

Actually, the same marching process is done from $x = L$ to $x = 0$ step by step. Finally, the matrices S_0 and Z_0 at $x = 0$ are obtained. Notice that the initial S_1 and Z_1 are gotten form the BC at $x = L$.

If $D(x)$ is symmetric, the wave field at $x = L$ is solved by

$$u = V_{0,m}Z_0V_{0,m}^{\mathrm{T}}u_0,$$

where u and u_0 are, respectively, the discrete fields of $u(L,z)$ and $u(0,z)$. Otherwise, it can be solved by

$$u = V_{0,m} Z_0 \widehat{V}^{\mathrm{H}}_{0,m} u_0.$$

5. Numerical results and discussion

In this section, some examples are solved to show the performance of the improved method. The equations are solved by formulas of Eqs. (34)–(39) together with Eq. (32). It is noticed that the results of Eqs. (34)–(39) together with Eq. (33) are much similar. They are omitted for conciseness.

The problems (1) with BCs (3) and (4) are denoted as Cases 1 and 2, respectively. For each case, both homogeneous and inhomogeneous media are considered. The homogeneous media are used to verify the validity of our method, because the exact solutions can be obtained.

For the homogeneous media, let

$$\kappa^2(x,z) = (1+\alpha\mathbf{i})\kappa_0^2;$$

and for the inhomogeneous media, let

$$\kappa^2(x,z) = (1+\alpha\mathbf{i})\kappa_0^2[1+0.05e^{-20(x/L-0.5)^2}\sin^2(\pi z)],$$

where $\kappa_0 = 10$, and α is an adjustable factor related to the absorbing strength. Moreover, $L = 10, n = 300$ and $m = 30$ for both cases.

The fields $u(x,z)$ at $x = L$ are calculated by different step sizes to illustrate the large step characteristic of the improved OMM. Relative error curves of $u(L,z)$ are also illustrated to show the convergent rate.

Case 1: Problem (1) with BCs (2) and (3).

Firstly, we consider the homogeneous media. The starting field at $x = 0$ is $u_0(z) = \sin(2\pi z)$, which is the third propagation mode. Then Case 1 has an exact solution

$$u(x,z) = e^{\mathbf{i}\lambda_3 x}\sin(2\pi z), \tag{41}$$

where $\lambda_3 = \sqrt{\kappa^2 - (2\pi)^2}$ is the third eigenvalue of Eqs. (5) and (6). The field in Eq. (41) is used for reference.

In Fig. 2, the numerical fields $u(L,z)$ with the step length $h = 1$ are plotted together with the exact field (41). In each sub-figure, one can hardly see the difference between the numerical fields and the exact solutions. The wave amplitudes attenuate when α increases, while their phases are same in the three sub-figures. This is reasonable because the media are homogeneous. It concludes that pretty good solutions have been obtained with $h = 1$. Since κ is constant, the relative errors don't change with h.

Secondly, we consider the inhomogeneous media. Its starting field at $x = 0$ is

$$u_0(z) = \sum_{j=1}^{7}\sin(m_j z_0)\sin(m_j z)/\sqrt{\kappa_0^2 - m_j^2}, \quad \text{for}$$
$$m_j = (j-1/2)\pi,\ z_0 = 0.65. \tag{42}$$

It is the same as that used in [5].

This problem doesn't have an exact solution. The numerical fields with step length $h = 1/128$ are calculated for reference. Then fields $u(L,z)$ with $h = 1$ and $h = 1/128$ are drawn in Fig. 3 when $\alpha = 0.01, 0.05$ and 0.1. The results are still satisfactory. In the sub-figures of Fig. 3, there are tiny differences. However, the wave phases change with α. This is different from the homogeneous case. In order to show the convergent rate, the relative error curve is plotted in Fig. 4(a) with $\alpha = 0.01$. Here $E(u_h) = \frac{\|u_r - u_h\|_2}{\|u_r\|_2}$, where u_r is

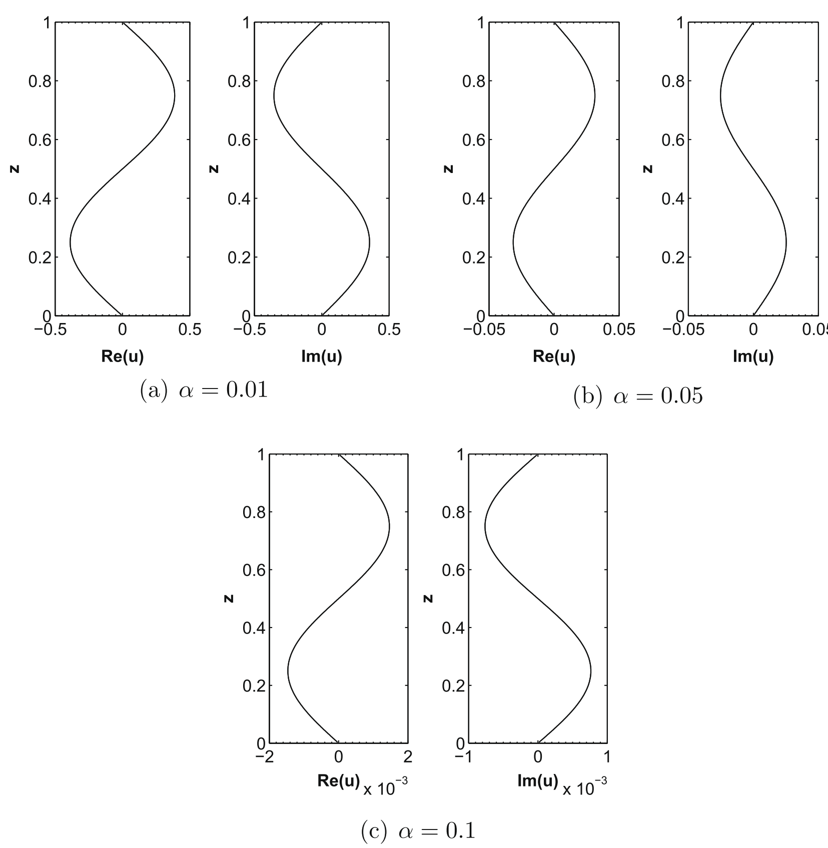

(a) $\alpha = 0.01$ (b) $\alpha = 0.05$ (c) $\alpha = 0.1$

Fig. 2. Fields $u(L,z)$ for Case 1: homogeneous media.

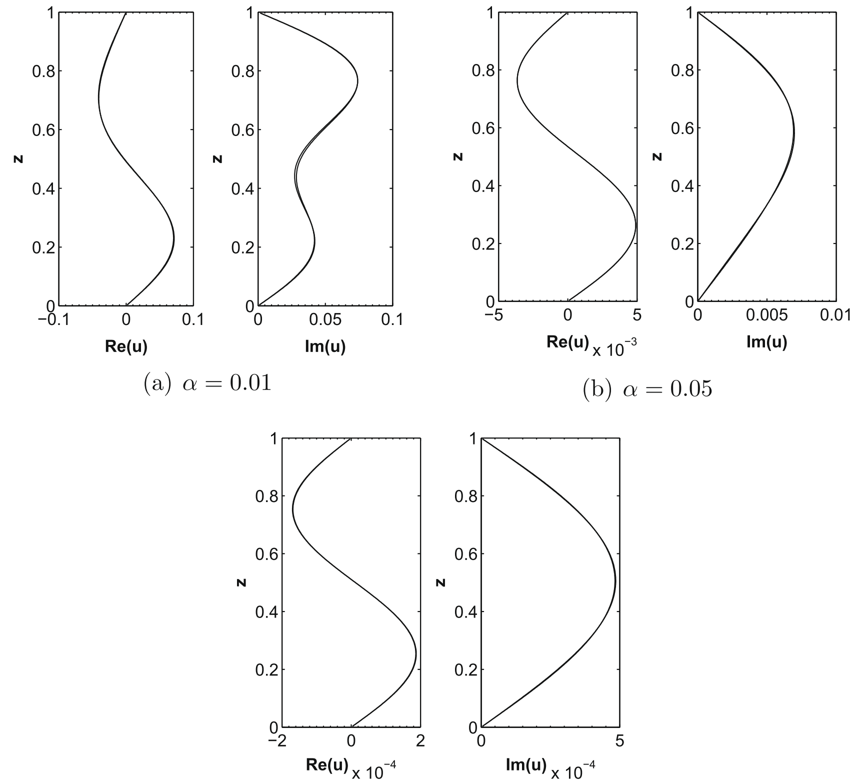

(a) $\alpha = 0.01$ (b) $\alpha = 0.05$

(c) $\alpha = 0.1$

Fig. 3. Fields $u(L,z)$ for Case 1: inhomogeneous media.

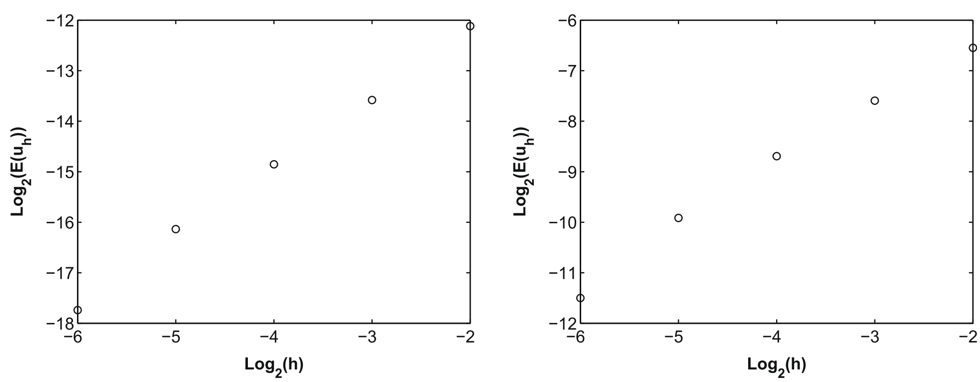

(a) Case 1 (b) Case 2

Fig. 4. Relative error curves of $u(L,z)$ for the two cases in inhomogeneous media ($\alpha = 0.01$).

the reference field with the step length $\frac{1}{128}$, u_h is the numerical field with the step length h, and $\|.\|_2$ denotes the 2-norm. The error curve demonstrates the method has second order accuracy.

Case 2: Problem (1) with BCs (2) and (4).

As known in Section 2, the complete basis property of D in Eqs. (5) and (7) is guaranteed by perturbation theory under the assumption of small $\mathrm{Im}(\kappa)$. Here $\alpha = 0.01, 0.05$ and 0.1 are studied.

Similar as Case 1, we consider the homogeneous media first. The starting field at $x = 0$ is $u_0(z) = \sin(2.5\pi z)$ corresponding to the third propagation mode of Eqs. (5) and (7). Then the problem in Eqs. (1) and (3) has an exact solution

$$u(x,z) = e^{\mathbf{i}\lambda_3 x}\sin(2.5\pi z), \tag{43}$$

where $\lambda_3 = \sqrt{\kappa^2 - (2.5\pi)^2}$ is the third eigenvalue. The field in Eq. (43) is used for reference in this case.

Numerical fields $u(L,z)$ with $h = 1$ as well as the reference fields in Eq. (43) are plotted in Fig. 5. The sub-figures, corresponds to the case of $\alpha = 0.01, 0.05$ and 0.1, respectively. In each figure, the waveforms of the numerical and the reference fields are almost coincident. Moreover, the wave phases do not change with α. It indicates good solutions have been obtained when $h = 1$.

In inhomogeneous media, assuming the starting field at $x = 0$ is same as Eq. (42), the field $u(L,z)$ is first calculated with $h = 1/128$ as a reference solution. The numerical fields $u(L,z)$ with $h = 1$ and the reference fields are both drawn in Fig. 6. Though it does not look so good as the forward cases, the results are still satisfactory. The relative error curve for this case with $\alpha = 0.01$ is drawn in Fig. 4(b). It indicates the improved OMM also has a second order accuracy.

In Table 1, the relative errors of $u(L,z)$ in inhomogeneous media are listed in order to show the influence of α on the solution accu-

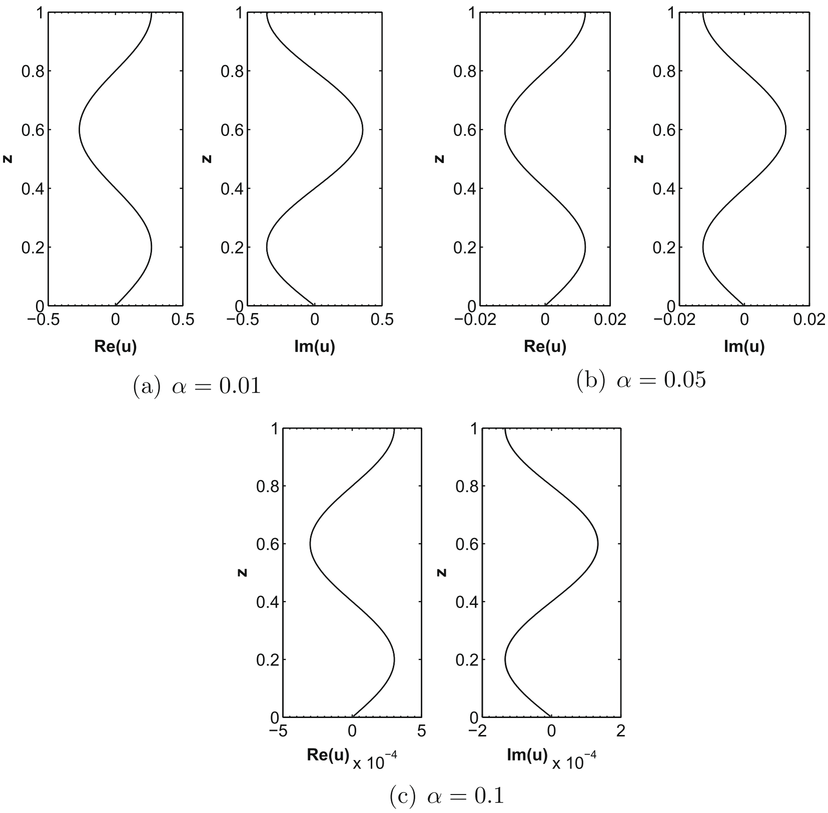

Fig. 5. Fields $u(L,z)$ for Case 2: homogeneous media.

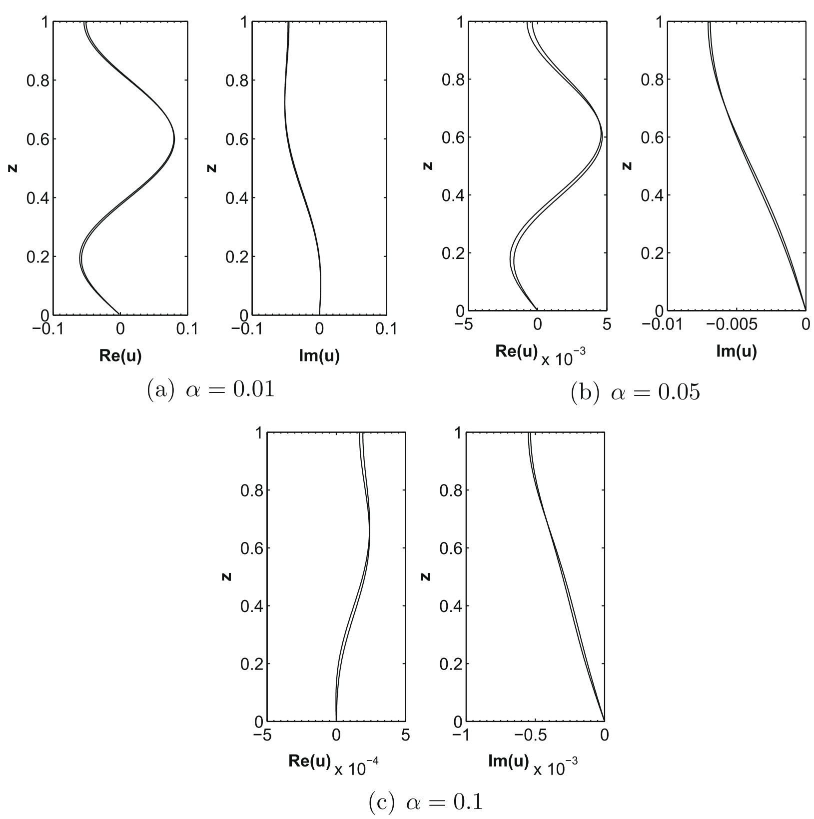

Fig. 6. Fields $u(L,z)$ for Case 2: inhomogeneous media.

racy. The relative errors of Case 1 decrease with α, while those of Case 2 almost remain unchanged. It shows that different α used in this study has little effect on the accuracy of solutions, although the errors of Case 1 are slightly smaller than those of Case 2 with

Table 1
Relative errors of $u(L,z)$ with different α in inhomogeneous media.

α	0.01	0.05	0.1
Case 1	1.7153×10^{-2}	9.8164×10^{-3}	6.4684×10^{-3}
Case 2	4.0967×10^{-2}	5.6159×10^{-2}	5.3891×10^{-2}

the same α. All these errors are acceptable. It indicates the improved OMM is not only useful for the weakly lossy waveguide ($\alpha = 0.01$), but also applicable for the waveguide with rather strong loss ($\alpha = 0.1$).

From the above numerical studies, we show that the improved OMM still has a second order accuracy for a large step size.

6. Conclusions

An improved operator marching method for lossy waveguides is given in this study. The numerical results show that it keeps the advantages of the method proposed in [5] such as the large range step and good stability. Particularly, the improved method is also feasible for lossless waveguides, which can be treated as a special case of lossy waveguides.

The improved OMM has a second order accuracy due to the piecewise approximation. It can be further improved if the fourth order method [11] is used. The application of the improved method to some complicated lossy waveguides such as curved multi-layer waveguides is also important. One treatment is to flatten the waveguide first by the local orthogonal transform [16,17], then the adjoint operator method is used to do the local base transform.

To sum up, the improved OMM is useful for the modeling and design of micro-optical waveguides for on-chip optical interconnects that realized with lossy materials such as silicon oxynitride. Actual application of the method is in progress and will be reported elsewhere.

Acknowledgements

The authors would like to thank the Editor and reviewers for their valuable suggestions to improve this paper. This work was supported by the Natural Science Foundation of China under grant No.10571162 and the Natural Science Foundation of Zhejiang Province under Grant No. Y605181.

References

[1] Wong H, Iwai H. The road to miniaturization. Phys World 2005;18(9):40–4.
[2] Wong H, Filip V, Wong CK, Chung PS. Silicon integrated photonics begins to revolutionize. Microelectron Reliab 2007;47:1–10.
[3] Wong CK, Wong H, Kok CW, Chan M. Silicon oxynitride prepared by chemical vapor deposition as optical waveguide materials. J Cryst Growth 2006;288:171–5.
[4] Wong CK, Wong H, Chan M, Kok CW, Chan HP. Minimizing hydrogen content in silicon oxynitride by thermal oxidation of silicon rich silicon nitride. Microelectron Reliab 2006;46:2056–61.
[5] Lu YY. One-way large range step methods for Helmholtz waveguides. J Comput Phys 1999;152:231–50.
[6] Hanson GW, Yakovlev AB. Operator theory for electromagnetics. New York: Springer-Verlag; 2001.
[7] Chew W. Waves and fields in inhomogeneous media. New York: Wiley-IEEE Press; 1999.
[8] Horn RA, Johnson CR. Matrix analysis. Cambridge: Cambridge University Press; 1985.
[9] Golub GH, Van Loan CF. Matrix computations. 3rd ed. Maryland: The Johns Hopkins University Press; 1996.
[10] Evans RB. A coupled mode solution for acoustic propagation in a waveguide with stepwise depth variations of a penetrable bottom. J Acoust Soc Am 1983;74(1):188–95.
[11] Lu YY. A fourth order derivative-free operator marching method for Helmholtz equation in waveguides. J Comput Math 2007;25(6):719–29.
[12] Kato T. Perturbation theory for linear operators. New York: Springer-Verlag; 1966.
[13] She SX. Propagation loss in metal-clad waveguides and weakly absorptive waveguides by a perturbation method. Opt Lett 1990;15(16):900.
[14] Hulse CA, Knoesen A. Iterative calculation of complex propagation constants of modes in multilayer planar waveguides. IEEE J Quantum Elect 1992;28(12):2682–4.
[15] Visser TD, Blok H, Lenstra D. Modal analysis of a planar waveguide with gain and losses. IEEE J Quantum Elect 1995;31(10):1803–10.
[16] Lu YY, Huang J, McLaughlin JR. Local orthogonal transformation and one-way methods for acoustic waveguides. Wave Motion 2001;34:193–207.
[17] Lu YY, Zhu J. A local orthogonal transform for acoustic waveguides with an internal interface. J Comput Acoust 2004;12(1):37–53.